EUMETSAT Satellite Application Facility on Climate Monitoring
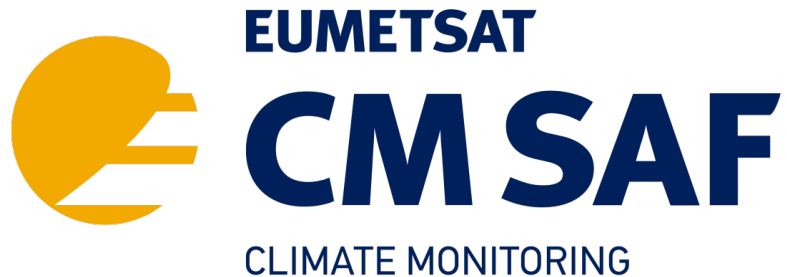
EUMETSAT
CM SAF
CLIMATE MONITORING

High-level Algorithm Theoretical Basis Document

SEVIRI cloud products

CLAAS Edition 3

	TCDR	ICDR
Fractional Cloud Cover (CFC)	**CM-21014**	**CM-5011**
Joint Cloud property Histogram (JCH)	**CM-21023**	**CM-5021**
Cloud Top level (CTO)	**CM-21033**	**CM-5031**
Cloud Phase (CPH)	**CM-21043**	**CM-5041**
Liquid Water Path (LWP)	**CM-21053**	**CM-5051**
Ice Water Path (IWP)	**CM-21063**	**CM-5061**

Document Signature Table

	Name	Function	Signature	Date
Author	Martin Stengel	CM SAF scientist		08/08/2022
	Irina Solodovnik	CM SAF scientist		
	Jan Fokke Meirink	CM SAF scientist		
	Nikos Benas	CM SAF scientist		
	Karl-Göran Karlsson	CM SAF scientist		
Editor	Marc Schröder	Science Coordinator CM SAF		08/08/2022
Approval	CM SAF Steering Group			
Release	Rainer Hollmann	Project Manager		

Distribution List

Internal Distribution	
Name	**No. Copies**
DWD / Archive	1
CM SAF Team	1

External Distribution		
Company	**Name**	**No. Copies**
Public		1

Document Change Record

Issue/ Revision	Date	DCN No.	Changed Pages/Paragraphs
3.0	14.12.2020	SAF/CM/DWD/ATBD/SEV/CLD 3.0	Initial version for CLAAS-3
3.1	19.02.2021	SAF/CM/DWD/ATBD/SEV/CLD 3.1	Updates following PCR RIDs

3.2	2005//2022	SAF/CM/DWD/ATBD/SEV/CLD 3.2	Updates for DRR/ORR, mainly reflecting differences between TCDR and ICDR
3.3	08/08/2022	SAF/CM/DWD/ATBD/SEV/CLD 3.3	Version after DR/ORR, with RID responses implemented

Applicable Documents

Reference	Title	Code
AD 1	EUMETSAT CM°SAF CDOP 3 Product Requirements Document (PRD)	SAF/CM/DWD/PRD, v.4.0

Reference Documents

Reference	Title	Code
RD 1	Algorithm Theoretical Basis Document for probabilistic cloud masking (CMa-prob)	NWC/CDOP3/PPS/SCI/ATBD/CloudProbability v2.0d
RD 2	Algorithm Theoretical Basis Document for Cloud Top Temperature, Pressure and Height of the NWC/PPS	NWC/CDOP3/PPS/SCI/ATBD/CTTH v3.0d
RD 3	Algorithm Theoretical Basis Document (An Appendix to the NWC/PPS) Cloud Probability and Cloud Top Temperature/Height from SEVIRI	SAF/CM/SMHI/ATBD/SEV/PPSSEV v3.2
RD 4	Algorithm Theoretical Basis Document Cloud Physical Products SEVIRI	SAF/CM/KNMI/ATBD/SEVIRI/CPP v3.2

Table of Contents

List of Tables

List of Figures

1   The EUMETSAT SAF on Climate Monitoring

The importance of climate monitoring with satellites was recognized in 2000 by EUMETSAT Member States when they amended the EUMETSAT Convention to affirm that the EUMETSAT mandate is also to "contribute to the operational monitoring of the climate and the detection of global climatic changes". Following this, EUMETSAT established within its Satellite Application Facility (SAF) network a dedicated centre, the SAF on Climate Monitoring (CM SAF, http://www.cmsaf.eu).

The consortium of CM SAF currently comprises the Deutscher Wetterdienst (DWD) as host institute, and the partners from the Royal Meteorological Institute of Belgium (RMIB), the Finnish Meteorological Institute (FMI), the Royal Meteorological Institute of the Netherlands (KNMI), the Swedish Meteorological and Hydrological Institute (SMHI), the Meteorological Service of Switzerland (MeteoSwiss), the Meteorological Service of the United Kingdom (UK MetOffice), and the Centre National de la Recherché Scientifique (CNRS). Since the beginning in 1999, the EUMETSAT Satellite Application Facility on Climate Monitoring (CM SAF) has developed and will continue to develop capabilities for a sustained generation and provision of Climate Data Records (CDRs) derived from operational meteorological satellites.

In particular the generation of long-term data sets is pursued. The ultimate aim is to make the resulting data sets suitable for the analysis of climate variability and potentially the detection of climate trends. CM SAF works in close collaboration with the EUMETSAT Central Facility and liaises with other satellite operators to advance the availability, quality and usability of Fundamental Climate Data Records (FCDRs) as defined by the Global Climate Observing System (GCOS). As a major task the CM SAF utilizes FCDRs to produce records of Essential Climate Variables (ECVs) as defined by GCOS. Thematically, the focus of CM SAF is on ECVs associated with the global energy and water cycle.

Another essential task of CM SAF is to produce data sets that can serve applications related to the new Global Framework of Climate Services initiated by the WMO World Climate Conference-3 in 2009. CM SAF is supporting climate services at national meteorological and hydrological services (NMHSs) with long-term data records but also with data sets produced close to real time that can be used to prepare monthly/annual updates of the state of the climate. Both types of products together allow for a consistent description of mean values, anomalies, variability and potential trends for the chosen ECVs. CM SAF ECV data sets also serve the improvement of climate models both at global and regional scale.

As an essential partner in the related international frameworks, in particular WMO SCOPE-CM (Sustained COordinated Processing of Environmental satellite data for Climate Monitoring), the CM SAF - together with the EUMETSAT Central Facility, assumes the role as main implementer of EUMETSAT's commitments in support to global climate monitoring. This is achieved through:

- Application of highest standards and guidelines as lined out by GCOS for the satellite data processing,
- Processing of satellite data within a true international collaboration benefiting from developments at international level and pollinating the partnership with own ideas and standards,

- Intensive validation and improvement of the CM SAF climate data records,

- Taking a major role in data set assessments performed by research organisations such as WCRP. This role provides the CM SAF with deep contacts to research organizations that form a substantial user group for the CM SAF CDRs,

- Maintaining and providing an operational and sustained infrastructure that can serve the community within the transition of mature CDR products from the research community into operational environments.

A catalogue of all available CM SAF products is accessible via the CM SAF webpage, www.cmsaf.eu/. Here, detailed information about product ordering, add-on tools, sample programs and documentation is provided.

2   Introduction

The third edition of the CLoud property dAtAset using SEVIRI (CLAAS-3) is a data record of cloud products derived from measurements taken by the Spinning Enhanced Visible and InfraRed Imager (SEVIRI) onboard the EUMETSAT Meteosat Second Generation (MSG) satellites. CLAAS-3 consists of a Thematic Climate Data Record (TCDR), spanning the period from 2004 to 2020, and an Interim Climate Data Record (ICDR), starting in 2021 and extended operationally with low latency to the present (see Figure 2-1). The ICDR is produced with the same algorithms as the TCDR but with a few differences in input data (see Section 4.7).
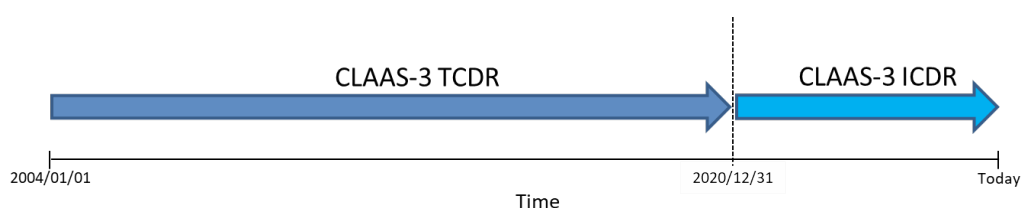
Figure 2-1: Illustration of the CLAAS-3 TCDR and ICDR temporal coverage.

This CM SAF Algorithm Theoretical Basis Document (ATBD) provides information on the processing algorithms and chain implemented for the generation of the CLAAS-3 cloud products, as successor of the CLAAS-2.1 record. The dataset contains retrieved geophysical parameters from inter-calibrated measurements of the SEVIRI instruments mounted on the MSG-1, MSG-2, MSG-3, and MSG-4 satellites. The cloud property algorithms applied are firstly the NWC/PPS version v2018 patch5 incl. CmsafPpsSeviri 0.5.0 software package (PPS hereafter) by the NWC SAF (SAF for support to Nowcasting and Very Short Range Forecasting) used to derive cloud fraction and cloud top properties ([RD 1], [RD 2] and [RD 3]). Secondly, CPP (Cloud Physical Properties) algorithm v6.0 ([RD 4]) was used, which retrieves cloud-top thermodynamic phase, cloud optical thickness, cloud particle effective radius, and liquid/ice water path.

The document seamlessly describes all elements of the production of the final CLAAS-3 cloud products, which are structured in the following three topics.

1. A description of the data sources and a summary of SEVIRI instrument characteristics are given, including a description of the inter-calibration applied to CLAAS-3 measurements.
2. A brief summary on the derivation of the Level-2 cloud products by applying PPS and CPP.
3. A report on the production of the daily and monthly means/histograms (Level-3 data) including a description of Level-2 uncertainty propagation into Level-3.

Product requirements are defined in the product requirements document [AD 1].

The CLAAS-3 data set contains the following cloud products:

	TCDR	**ICDR**
Fractional Cloud Cover (CFC)	**CM-21014**	**CM-5011**
Joint Cloud property Histogram (JCH)	**CM-21023**	**CM-5021**
Cloud Top level (CTO)	**CM-21033**	**CM-5031**
Cloud Phase (CPH)	**CM-21043**	**CM-5041**
Liquid Water Path (LWP)	**CM-21053**	**CM-5051**
Ice Water Path (IWP)	**CM-21063**	**CM-5061**

3 Processing of measured SEVIRI radiances (Level-1.5)

3.1 The SEVIRI instrument

SEVIRI is a passive optical imaging radiometer with 12 spectral channels at visible and infrared wavebands. SEVIRI instruments are mounted on the geostationary MSG satellites and measure from 2004 onwards. MSG 1, MSG 2, MSG 3 and MSG 4 measurement images are made to align to each other and centred at 0°/0° longitude/latitude. The region seen by a SEVIRI instrument is shown in Figure 5-1. It covers Africa, Europe, partly South America, the Atlantic Ocean and the Middle East. In Figure 3-1 the time-span of CLAAS-3 is displayed together with separation of available MSG 1, MSG 2, MSG 3 and MSG 4 measurements, also indicating gaps during the operation. All four SEVIRI instruments on MSG 1, MSG 2, MSG 3 and MSG 4 are identical in construction. Table 3-1 lists the main characteristics of the SEVIRI instrument. The SEVIRI measurement principle is explained in the following.

An MSG satellite spins around its vertical axis with 100 rotations per minute, the SEVIRI instrument uses this spin to scan the earth line-by-line in east-west direction. After each line, the scan mirror is moved one step in South-North direction and the next line is scanned. The acquisition time of one image is 12 minutes, together with onboard calibration and scan mirror retrace a nominal repeat cycle of 15 minutes is achieved.

For each of the 12 spectral channels three detectors acquire three lines of an image simultaneously. The HRV channel however has 9 detectors and 9 lines are obtained per revolution. In Table 3-2 SEVIRI's channels and their characteristics can be found. After each scan a black body calibration is applied for the infrared channels as well as a measurement of the deep space radiance. The deep space radiance corresponds to zero input radiance and is subtracted from the measured signal. The black body calibration is undertaken by moving a black body into the telescope in the intermediate focal plane. The accuracy of SEVIRI was determined prior to the launch in space. The infrared channels measure brightness temperature with a precision of < 1 K for a target of 300 K while the noise for the shortwave channels ranges from 0.08 to 0.52 W/(m² sr µm), for more details see Table 3-3.

After acquiring an image, the data are sent to the EUMETSAT ground segment where they are further processed into Level 1.5 data as described in section 4. After this processing step the images are ready to be disseminated to the user.

Table 3-1: SEVIRI instrument features.

SEVIRI instrument features.
line-by-line scanning radiometer
12 spectral channels 0.6 -13.4 µm, image every 15 min.
Scan duration 12 min.
blackbody calibration for thermal channels at every scan (15 min.)
spatial resolution: 3 km at sub-satellite point (1 km for HRV)

radiometric noise: <1 K for IR and 0.08 – 0.52 W m^{-2} sr^{-1} μm^{-1} for SW channels

Table 3-2: SEVIRI channel characteristics (source: EUMETSAT, 2017)

Channel ID	Absorption Band / Channel Type	Nominal Centre Wavelength (μm)	Spectral Bandwidth (μm)	Dynamic Range	Spectral Bandwidth As % of energy actually detected within spectral band
HRV	Visible High Resolution	Nominally 0.75	0.6 to 0.9	0 - 459 W/m2 sr μm (scaled at centre frequency)	Precise spectral characteristics not critical
VIS 0.6	VNIR Core Imager	0.635	0.56 to 0.71	0 - 533 W/m2 sr μm	98.0 %
VIS 0.8	VNIR Core Imager	0.81	0.74 to 0.88	0 - 357 W/m2 sr μm	99.0 %
IR 1.6	VNIR Core Imager	1.64	1.50 to 1.78	0 - 75 W/m2 sr μm	99.0 %
IR 3.9	IR / Window Core Imager	3.92	3.48 to 4.36	0 - 335 K	98.6 %
IR 6.2	Water Vapour Core Imager	6.25	5.35 to 7.15	0 - 300 K	99.0 %
IR 7.3	Water Vapour Pseudo-Sounding	7.35	6.85 to 7.85	0 - 300 K	98.0 %
IR 8.7	IR / Window Core Imager	8.70	8.30 to 9.10	0 - 300 K	98.0 %
IR 9.7	IR / Ozone Pseudo-Sounding	9.66	9.38 to 9.94	0 - 310 K	99.0 %
IR 10.8	IR / Window Core Imager	10.80	9.80 to 11.80	0 - 335 K	98.0 %
IR 12.0	IR / Window Core Imager	12.00	11.00 to 13.00	0 - 335 K	98.0 %
IR 13.4	IR / Carbon Dioxide Pseudo-Sounding	13.40	12.40 to 14.40	0 - 300 K	96.0 %

Table 3-3: SEVIRI channel noise budgets expressed in K for IR channels and W/(m² sr μm) for shortwave channels as reported in Schmid (2000)

Channel (μm)	HRV	0.6	0.8	1.6	3.9	6.2	7.3	8.7	9.7	10.8	12.0	13.4
Noise	0.52	0.39	0.36	0.08	0.24	0.40	0.48	0.15	0.24	0.13	0.21	0.29

Spec.	1.07	0.53	0.49	0.25	0.35	0.75	0.75	0.28	1.50	0.25	0.37	1.80

3.2   The SEVIRI measurement record

The SEVIRI measurement record spans the time-period from 2004 onwards, measurements from the respective instrument on the satellite that was in operational mode was used. During the time-span of CLAAS-3, three operational changes took place, one from MSG 1 to MSG 2 in 2008, from MSG 2 to MSG 3 in 2013 and from MSG 3 to MSG 4 in 2018.

In this edition of the dataset (CLAAS-3) SEVIRI's native temporal resolution of 15 minutes and horizontal resolution of 3 x 3 km² at nadir are utilized. CLAAS-3 covers the time-span Jan. 2004 to Dec. 2020, where MSG1 measurements were processed from 01/2004 to 04/2007, MSG 2 measurements from 04/2007 to 01/2013, MSG 3 measurements from 01/2013 to 19/02/2018 and MSG 4 measurements from 20/02/2018 onwards. Gaps of more than 24 hours in the time-series of the operational satellite were filled with backup measurements (Figure 3-1); exact dates with gaps and missing dates in the MSG record that could be filled with measurements of the backup satellite are listed in Table 3-4.

For the derivation of the cloud products the Level 1.5 SEVIRI data provided by EUMETSAT were used. Level 1 data is image data that was directly transferred to the EUMETSAT's ground segment. i.e. raw data before any modification has taken place. The Level 1.5 data record comprises image data that has already undergone certain modifications by EUMETSAT: it has been corrected for all unwanted radiometric and geometric effects, has been geolocated using a standardised projection, and has been calibrated and radiance-linearised.
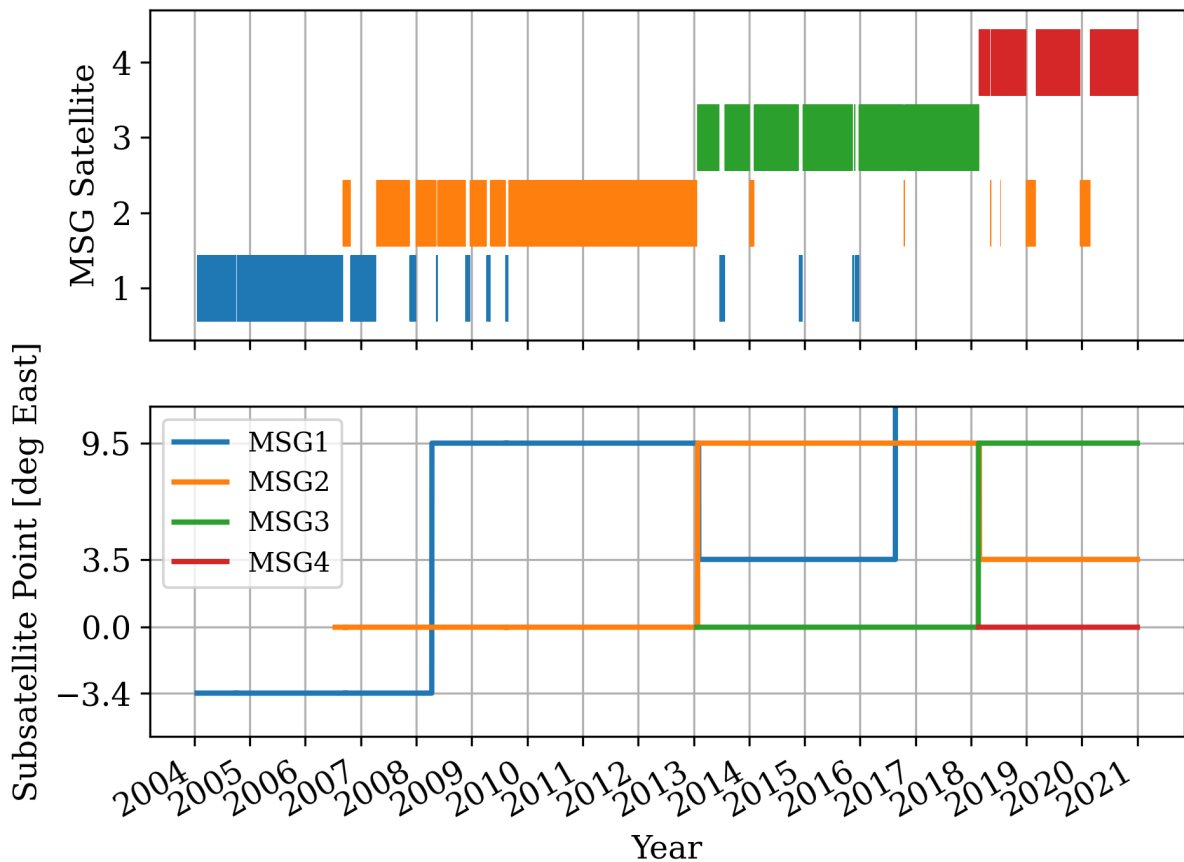
Figure 3-1: Overview of SEVIRI measurements record used as basis for the generation of CLAAS-3. Data gaps > 1 day are shown enlarged by a factor 5 for better visibility. MSG-1 was re-located to 41.5° East in August 2016.

Some of the processing steps are described in the following: First, the raw data are projected onto the SEVIRI disk to form a geolocated image. Every image (except for HRV, which will not be described further, since its measurements are not used for CLAAS-3) consists of 3712 lines by 3712 columns. The space area of the Level 1.5 image is set to a predefined binary value, also the missing pixel will be replaced by this value. The sampling distance is defined to be exactly 3 km by 3 km at the sub-satellite point and the geolocation is centred at 0° latitude and 0° longitude where the centre is situated in the middle of the pixel with the line numbers (1856,1856).

The image data are stored in a 10 bit integer format, and therefore have been scaled. The user has to apply the gain and offset given in the header to receive the actual radiance values. Please note that EUMETSAT introduced a new radiance definition, changing from spectral radiance to effective radiance, in 2008 (see EUMETSAT, 2008). The whole SEVIRI Level 1.5 data archive was reprocessed by EUMETSAT and the new files were transferred to the DWD, so the complete CLAAS-3 dataset relies on the reprocessed Level 1.5 radiances.

Table 3-4: Gaps in SEVIRI measurement record of the prime MSG satellites. Gaps shorter than 1 day are not listed. Last column lists the backup satellites (if available) whose data is used to fill the gaps for CLAAS-3.0. Time period considered is Jan. 2004 to Dec. 2020.

Gaps in operational service of the prime MSG satellites		Prime satellite	Replacement
from	to		
05/10/2004	06/10/2004	MSG-1	no
24/09/2006	24/09/2006	MSG-1	no
25/09/2006	05/10/2006	MSG-1	MSG-2
04/12/2007	12/12/2007	MSG-2	MSG-1
14/05/2008	16/05/2008	MSG-2	MSG-1
02/12/2008	08/12/2008	MSG-2	MSG-1
18/04/2009	23/04/2009	MSG-2	MSG-1
16/08/2009	16/08/2009	MSG-2	no
17/08/2009	21/08/2009	MSG-2	MSG-1
02/07/2013	09/07/2013	MSG-3	MSG-1
15/01/2014	21/01/2014	MSG-3	MSG-2
03/12/2014	08/12/2014	MSG-3	MSG-1
16/11/2015	18/11/2015	MSG-3	MSG-1
09/12/2015	14/12/2015	MSG-3	MSG-1
16/10/2016	17/10/2016	MSG-3	MSG-2
20/02/2018	20/02/2018	MSG-4	MSG-3
07/05/2018	08/05/2018	MSG-4	MSG-2
11/07/2018	11/07/2018	MSG-4	MSG-2
22/01/2019	04/02/2019	MSG-4	MSG-2

Until 2017-12-06, SEVIRI level 1.5 images were shifted by 1.5km (at nadir) North and West against the nominal GEOS projection due to various small errors in the ground processor (see EUMETSAT, 2017, section 3.1.4.2). The georeferencing offset was corrected by EUMETSAT on 2017-12-06. Level 2 products contain a flag which indicates if the correction has been applied. To make data and coordinates always matching accurately level 2 products are provided on the shifted grid before 2017-12-06, and in the nominal GEOS projection after that date. As a result, two sets of auxiliary data will be provided.

3.3 Applied SEVIRI solar channel calibration description

SEVIRI does not carry an on-board calibration device for the solar channels. Therefore, EUMETSAT operates a vicarious calibration system using Earth targets (desert and ocean) as reference. Analyses by Doelling et al. (2004) and Ham and Sohn (2010) revealed that the resulting visible channel nominal calibration, provided in the SEVIRI Level-1.5 data files, has a considerable offset with respect to the Moderate Resolution Imaging Spectroradiometer (MODIS), which is thought to be a well-calibrated reference instrument. Meirink et al. (2013) extended these previous analyses to the NIR channels and to longer time periods. They used collocated, ray-matched, atmosphere-corrected, near-nadir SEVIRI and Aqua-MODIS reflectances to derive inter-calibration slopes, i.e. multiplicative factors to be applied to SEVIRI

nominal reflectance in order to match the MODIS measurements. This calibration work was extended to cover the full CLAAS-3 time window of 2004 to 2020, including all four SEVIRI instruments that have been active. The same method was applied as described in Meirink et al. (2013) but now using MODIS Collection 6.1 instead of Collection 5 Level-1b data as a reference. Results are shown in Figure 3-2.The operational MSG-SEVIRI calibration is biased low for channels 1 and 2, but biased high for channel 3. Furthermore, the comparisons with MODIS demonstrate that the SEVIRI calibration coefficients change significantly over time for channels 1 and 2, which needs to be taken into account. Thus, for CLAAS-3 processing the calibration slopes shown by the solid lines in Figure 3-2 will be used. Note that for the longwave, thermal infrared channels the operational calibration provided in the SEVIRI level 1.5 files is adopted as is.
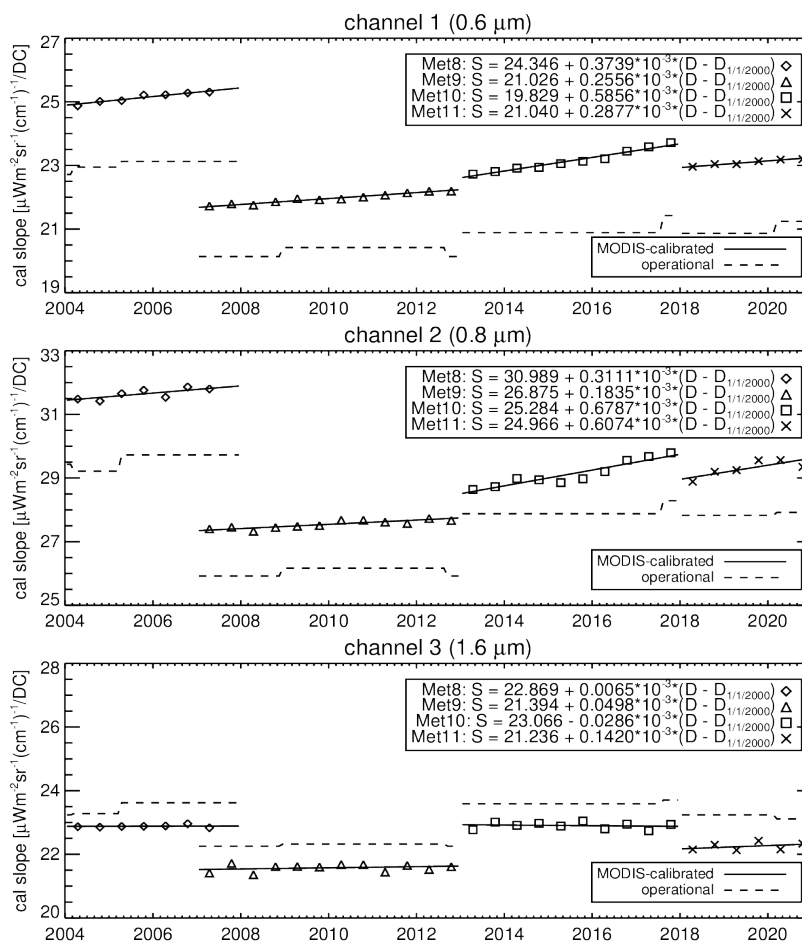

Figure 3-2: Time series of MSG-SEVIRI calibration slopes for the three solar channels as derived operationally by EUMETSAT (dashed) and from inter-calibration with Aqua-MODIS (symbols and solid line fits). The fit coefficients are indicated in the plots, with $D - D_{1/1/2000}$ being the number of days since 1 January 2000.

4 Retrieval of pixel-based cloud properties (Level-2)

This section provides brief information on the processing of PPS and CPP to retrieve cloud properties from inter-calibrated SEVIRI measurements. Each property is briefly introduced in the following subsections with the respective detailed ATBD being referred to.

4.1 Fractional Cloud Cover [CM-21014/CM-5011, CFC]

This product is a result of the PPS probabilistic cloud masking procedure based on Bayesian theory. Individual measurement features, e.g. reflectance at 0.63 µm, are linked to the likelihood of being cloudy, which is inferred from a reliable reference, i.e. the Cloud-Aerosol Lidar with Orthogonal Polarization (CALIOP) in this case. The probabilities of being cloudy for all individual features are multiplied (assuming no correlations) to infer the total probability of a pixel being cloudy. One of the recently introduced key features is that the cloud probabilities are derived scene-dependently. The training of CMA-prob is based on SEVIRI-collocations with CALIPSO-CALIOP where data has been collected and sub-divided over 28 different surface types (see Table 2 in Karlsson et al. (2020) for surface type definition). Consequently, 28 different statistical distributions if image feature behaviour for cloudy and clear conditions is then used when executing CMA-prob. This accounts for scene-dependent variation in detection skills of passive satellite sensors and supports the general application globally of a 50% probability threshold to distinguish cloudy and clear-sky scenes without scene-dependent biases in detection skill. All downstream retrievals of the other cloud properties described in the following subsections are done in cloudy pixels only, identified by applying the 50% threshold. More information on the cloud detection schemes can be found in [RD 1] with SEVIRI specific adaptations given in [RD 3]. The reader is also referred to Karlsson et al. (2015, 2020).

The cloud fractional cover is defined as the fraction of cloudy pixels (applying 50% threshold, see above) per grid cell compared to the total number of analyzed pixels in the grid cell, i.e. all pixels that have a cloud probability assigned. Fractional cloud cover is expressed in percent.

4.2 Joint Cloud property Histogram [CM-21023/CM-5021, JCH]

The JCH product is a combined histogram of CTP (see Section 4.3), COT (see Sections 4.5 and 4.6), and CPH (see Section 4.4), covering the solution space of these parameters. This three-dimensional histogram gives the absolute numbers of occurrences for specific COT-CTP-CPH combinations defined by specific bins, which can be found in section 5.2.2.

4.3 Cloud Top level [CM-21033/CM-5031, CTO]

This product is based on the PPS neural network (of the type multilayer perceptron) trained offline with collocations of passive imager measurements and CALIOP (version 4 data) cloud top pressure observations. Training was performed using collocations over the full MSG disk, thus covering all variations caused by varying viewing angles. Collocated Numerical Weather

Prediction (NWP) profiles are used to convert cloud top pressure to cloud top temperature and height. The latter is expressed as altitude above ground topography.

In addition to the retrieved values (direct output of the neural network), the upper and lower boundaries are produced using a version of Quantile Regression Neural Networks (see Pfreundschuh et al. 2018). The actually reported CTTH uncertainties are processed by averaging the distances of both boundaries to the retrieved value to present a 68% confidence interval around the retried value.

More information on the PPS CTTH retrieval can be found in [RD 2] with SEVIRI specific adaptations given in [RD 3]. The reader is also referred to Håkansson et al. (2018) for more information.

4.4   Cloud Phase [CM-21043/CM-5041, CPH]

The cloud phase product is meant to represent the thermodynamic phase of the particles near the cloud top. The cloud-top phase retrieval is based on a number of threshold tests using SEVIRI channels IR_6.2, IR_8.7, IR_10.8, IR_12.0, and IR_13.4, while also consistency with the cloud optical thickness and particle effective radius retrieval from either the VIS_0.6-IR_1.6 or VIS_0.6-IR_3.9 channel combinations is demanded. Some of the tests involve clear and cloudy-overcast radiances, which are calculated using RTTOV. The algorithm is run for cloudy pixels and initially yields one of the following cloud types (also referred to as 'extended cloud phase'): liquid water, supercooled water, opaque ice, cirrus, overlap (ice above liquid), and overshooting convection (ice). These are then further condensed to liquid (former two) and ice (latter four) phase. Both the extended and the condensed phase are included in the output products. Details on the algorithm can be found in [RD 4].

4.5   Liquid Water Path [CM-21053/CM-5051, LWP]

For pixels to which the liquid phase has been assigned, liquid water path (LWP) is derived from the cloud optical thickness (COT or τ) and particle effective radius (CRE or r_e). The τ - r_e retrieval scheme, developed at KNMI, uses a pair of satellite radiances at wavelengths in the non-absorbing (for clouds) visible and the moderately absorbing solar infrared part of the spectrum, following methods introduced by, e.g., Nakajima and King (1990). The observed radiances are iteratively matched with values simulated with the Doubling Adding KNMI (DAK, De Haan et al., 1987) radiative transfer model and stored in lookup tables (LUTs), yielding τ between 0.1 and 150 and r_e between 3 and 34 µm. Scattering properties were calculated with Mie theory for spherical droplets. Two sets of retrievals are generated: one using the SEVIRI channels VIS_0.6 and IR_1.6 and one using channels VIS_0.6 and IR_3.9. Maximum solar and satellite zenith angles for which retrievals are performed are 84 degrees.

Liquid water path is then computed from the retrieved τ and r_e values as in Stephens (1978): LWP = 2/3 ρ_l τr_e, where ρ_l represents the density of liquid water (1000 kg m^{-3}). In addition, also the cloud droplet number concentration (CDNC) and the cloud geometrical thickness (CGT) are estimated following Bennartz and Rausch (2017). More details on the retrieval scheme can be found in [RD 4].

The level-2 product files do not only contain LWP but also COT, CRE, CDNC, and CGT as additional layers. Moreover, uncertainty estimates of these parameters are given.

4.6 Ice Water Path [CM-21063/CM-5061, IWP]

For pixels to which the ice phase has been assigned, ice water path (IWP) is retrieved in the same way as LWP described in Section 4.5. Here, the scattering properties were calculated based on severely roughened compact aggregates of solid columns (Yang et al., 2013; Baum et al., 2011), with effective radii between 5 and 60 μm and size distributions with an effective variance of 0.1. IWP is then computed with the same formula as LWP but with the density of ice (930 kg m^{-3}). More details on the retrieval scheme can be found in [RD 4]. As for LWP, COT and CRE are provided as additional layers in the product files, and error estimates of these parameters are given.

4.7 Ancillary, auxiliary and NWP data

Supporting the retrieval algorithms, a selected set of external data is utilized spanning surface albedo, surface emissivity, NWP thermodynamic profiles and surface data, sea-ice/snow-cover information, and calibration coefficients for the SEVIRI shortwave channels. Table 4-1 gives an overview of the external data used for the TCDR and ICDR. More detailed information can be found in [RD 3] and [RD 4].

Table 4-1: Summary of external data used as input to the retrieval algorithms and how they deviate between TCDR and ICDR. ERA5 is the ECMWF Re-Analysis 5 and ERA5T its low-latency version. OSI SAF is the Satellite Application Facility on Ocean and Sea Ice.

	TCDR	**ICDR**
Surface albedo	based on snow-including MODIS 'original' data + gap-filling	based on snow-free gap-filled MODIS data + aggregated and complemented with ERA5T snow information
Surface emissivity	Monthly climatologies based on MODIS	Monthly climatologies based on MODIS
NWP data	ERA5 skin temperature and profiles of temperature, moisture, geopotential height Snow cover information (interpreted from snow depth)	ERA5T skin temperature and profiles of temperature, moisture, geopotential height Snow cover information (interpreted from snow depth)
sea-ice	OSI-SAF-450 product and its extension OSI-430b and ERA5	near-realtime product OSI-401b and ERA5T
SEVIRI shortwave channel calibration coefficients	time dependent coefficients from temporal fits as outlined in Section 3.3	time dependent coefficients from continuation of the

		temporal fits in Section 3.3 beyond the TCDR period

5   Generation of daily and monthly means, and histograms (Level-3)

In addition to the Level 2 pixel-level products, which are on native SEVIRI projection and resolution, CLAAS-3 will also contain Level 3 products of various parameters and parameter combinations. The pixel-level Level-2 retrieval results of PPS and CPP are input to the L2/L3 processing. The L3 outputs are fields of daily and monthly averages (and histograms) summarized in Table 5-1 and their specification were defined in [AD 1]. These specifications are summarized in section 5.1.

Table 5-1: Summary of Level-3 products including day and night separation, liquid water and ice as well as histogram representation. Please note that the LWP and IWP histograms are combined in one product (CWPmh)

	Daily mean	Monthly mean	Monthly mean diurnal cycle	Monthly histograms
CFC	✓ day/night high/mid/low	✓ day/night high/mid/low	✓	
CTO	✓ day/night liquid/ice	✓ day/night liquid/ice	✓	✓
CPH	✓ day/day+night	✓ day/day+night	✓	
LWP (+τ, r_e, CDNC, CGT)	✓	✓	✓	✓
IWP (+τ, r_e)	✓	✓	✓	✓
JCH				✓ liquid/ice

The covered geographic area is shown in Figure 5-1. The Level 2 data pixels are projected onto a regular latitude/longitude grid with a resolution of 0.05 x 0.05 degree^2 and both collected in daily histograms as well as averaged to daily means. An exception is the JCH for which the lat/lon resolution is 0.25 x 0.25 degree^2 because of the need to get enough statistical samples for the product to give representative results. The daily means/histograms are then further processed to monthly means/histograms with each daily data being weighted equally.
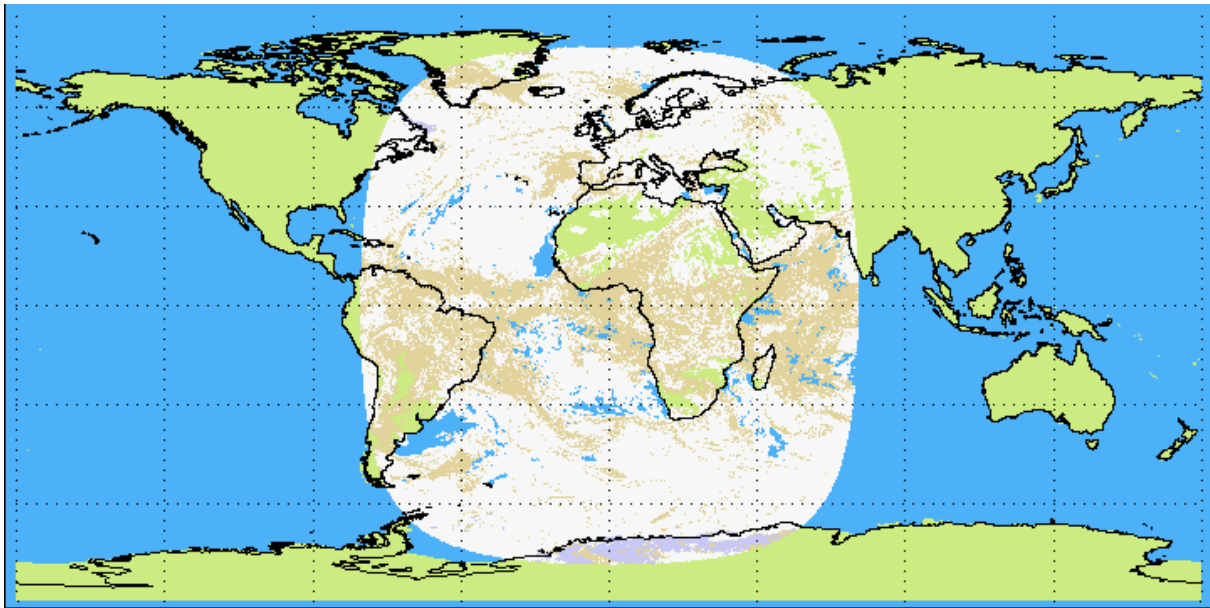
Figure 5-1: Area seen by SEVIRI. Example is for cloud fractional cover.

5.1   Definition of product specifications

The CLAAS-3 cloud data set provides a number of cloud parameters on the area indicated in Figure 5-1. Instantaneous retrievals with a temporal resolution of 15 minutes at original spatial resolution are used to derive the spatio-temporally collected data sets. The products are available as daily mean as well as monthly means/histograms on a regular latitude/longitude grid with a spatial resolution of 0.05 × 0.05 degrees². Also, monthly mean diurnal cycles are generated consisting of 24 time-steps with a spatial resolution of 0.25 × 0.25 degrees². The data of each of the 24 time steps is calculated by averaging all 4 time slots of a particular hour ('00,'15,'30,'45) over all days of a month.

Acknowledging the different observation capabilities during night and during day and also taking into account existing diurnal variations in cloudiness, a further separation of results in daytime and night-time portions has also been done (for fractional cloud cover, cloud top level and cloud phase). Here, all observations made under twilight conditions (solar zenith angle between 75° and 95°) have been excluded in order to avoid being affected by specific cloud detection problems occurring in the twilight zone.

In addition to the mean values, histograms are provided on monthly time scales. The Joint Cloud property Histograms are three-dimensional histograms of CPH, COT and CTP, and are composed with a spatial resolution of 0.25 x 0.25 degrees². (See Section 5.3.2 for more technical details). For CTP, CTT, COT, CRE, CWP, CPH, CDNC and CGT one-dimensional histograms are constructed on a monthly basis with a spatial resolution of 0.05 × 0.05 degrees². CTP, CTT, COT, CRE, CWP histograms provide separate information for liquid and ice clouds, CDNC and CGT only for liquid clouds. CPH histograms allocate the occurrence of different cloud types (see Sections 5.3.3, 5.3.4, 5.3.6 and 5.3.7 for more technical details).

5.2   Calculation of Level 3 products

For the daily averages/histograms all data fields with original SEVIRI pixel size in 15 minutes resolution are temporally averaged and collected. Here, all values are considered equally valid, thus no weighting is applied. Monthly means/histograms are generated from daily data.

It is important to note that different quality checks are applied for filtering valid numbers for each parameter. This is motivated by the fact that not in all cases where a cloud mask is available all cloud retrieval results of CPH, CTO, COT, CRE, LWP, IWP, CDNC and CGT are available. The specifics for filtering are summarized in Table 5-2. and also detailed in the following subsections.

Table 5-2: Overview of filtering applied for the derivation of L3 from L2 products.

Product	Filtering	Explanation
All daytime products (CFC day, CTH/CTP/CTT day, CPH day, LWP (and sub-products), IWP (and sub_products), JCH	solar zenith angle < 75°	Definition of daytime (avoid low solar elevations because of potential retrieval problems
All nighttime products (CFC night, CTH/CTP/CTT night, CPH night)	solar zenith angle > 95°	Definition of nighttime (avoid twilight conditions)
CFC low	CTP > 680 hPa	ISCCP definition of low-level clouds
CFC middle	440 hPa < CTP < 680 hPa	ISCCP definition of mid-level clouds
CFC high	CTP < 440 hPa	ISCCP definition of high-level clouds
CPH day, LWP (and sub-products), IWP (and sub-products)	*Exclude* pixels satisfying ALL following conditions: - surface type is water - scattering angle differs less than 27° from direct glint angle - satellite viewing zenith angle > 30°	Avoid possibly sunglint-affected conditions, which mainly give a risk of erroneous cloud optical/microphysical retrievals at higher viewing zenith angles
CRE (liquid and ice), CDNC (liquid), CGT (liquid)	*Exclude* pixels with CRE retrieval outside look-up table	Avoid these flagged L2 retrievals to enter L3. Note: corresponding LWP, IWP and COT retrievals are not excluded.

5.2.1 Fractional Cloud Cover [CFC]

The Fractional Cloud Cover product contains mean fractional cloud cover *CFC* and mean probabilistic cloud mask *CMA_PROB*.

The daily mean probabilistic cloud mask is a result of the temporal averaging of probabilistic cloud mask values. All valid entries of the original fields are aggregated and then weighted by the number of cloudy and clear cases.

The daily mean fractional cloud cover is calculated from the aggregation of the instances of the binary cloud mask information (after applying a 50% threshold to the probabilistic clouds mask) as follows:

Equation 5-1

$$CFC(i,j) = \frac{N(i,j)_{Cloudy}}{N(i,j)_{Cloudy} + N(i,j)_{Clear}}$$

with i and j being the indices of the original field projection, $N(i,j)_{Cloudy}$ the number of cloudy cases and $N(i,j)_{Clear}$ the number of clear cases.

Acknowledging the different cloud detection capability during day and night time, an additional separation is done leading to separate day time and night time averages for CFC and CMA_PROB. Here, the solar zenith angle of ≤75° and ≥95° are used to define day and night, respectively. Cases with solar zenith angles between 75° and 95° are included in the nominal daily mean but excluded when collecting data for day-only and night-only averages. Mean fractional cloud cover in pre-defined vertical layers is also provided separately. This is calculated in different pressure intervals, which are defined by Cloud Top Pressure. CFC_low for CTP > 680 hPa, CFC_middle for 440 hPa < CTP < 680 hPa, CFC_high for CTP < 440 hPa.

The monthly mean cloud fractional cover and mean probabilistic cloud mask are calculated as mean over the daily means with each day being weighted equally.

5.2.2 Joint Cloud property Histogram [JCH]

The JCH does not include a classical mean of a specific cloud property but covers the solution space for the 3 cloud parameters: COT, CTP and CPH. Hence, the JCH product is only available for daytime observations, defined as observations with solar zenith angle lower than 75°. This product is described in a five-dimensional field *JCH(i,j,τ,p,ph)*. Indices i and j refer to location space, while τ and p being the indices for specific bins of the range of occurring COT and CTP values, and *ph* denotes the cloud phase.

Each specific field entry contains the absolute number of cloud pixels with phase *ph* falling into the COT bin τ and the CTP bin p. The following values bordering the bins of COT and CTP (given in hPa) have been defined:

COT:{ 0, 0.3, 0.6, 1.3, 2.2, 3.6, 5.8, 9.4, 15, 23, 41, 60, 80, 149.99, inf} and

CTP:{ 1, 90, 180, 245, 310, 375, 440, 500, 560, 620, 680, 740, 800, 875, 950, 1100} [hPa].

Note that, while in the L2 output, COT values are maximized at 150, this variable can in principle take arbitrarily large values, which is reflected by setting the upper bound in the histogram to infinity.

5.2.3 These histograms are calculated for liquid and ice clouds separately. Cloud Top Level [CTO]

The CTO product contains daily means for CTH, CTP, and CTT. For these parameters all valid entries of the original fields are aggregated and then weighted by the number of used entries.

Equation 5-2
$$< x(i,j) > = \frac{1}{N(i,j)_{Cloudy}} \sum_{k=1}^{N(i,j)_{Cloudy}} x_k(i,j)$$

with $x(i,j)$ being a general expression for CTH, CTP and CTT at a specific original grid cell.

After temporal averaging, the fields are remapped to the final resolution as described in section 5.1.

For CTP, an alternative way of averaging is followed and additionally calculated and provided as geometrical mean where the variables are averaged in logarithm space:

Equation 5-3
$$< ctp(i,j) >_{ln} = \exp(\frac{1}{N(i,j)_{Cloudy}} \sum_{k=1}^{N(i,j)_{Cloudy}} \ln(ctp_k(i,j)))$$

Geometrical mean is added to keep consistency between CTH and CTP. CTP depends logarithmically on CTH, so if CTH is averaged linearly, CTP has to be averaged logarithmically to preserve the relation.

An additional separation due to the cloud thermodynamic phase as well as between day and night leads to four further variables: $<x(i,j)>_{liq\_day}$, $<x(i,j)>_{ice\_day}$, $<x(i,j)>_{liq\_night}$, $<x(i,j)>_{ice\_night}$. The cloud thermodynamic phase is defined by CPH product, daytime corresponds to solar zenith angle lower than 75°, night-time - higher than 95°.

The monthly mean cloud top level parameters are calculated as mean over the daily means with each day being weighted equally.

One-dimensional monthly histograms are generated for CTP and CTT on the same spatial resolution, but only on monthly basis. The bin borders for these histograms are:

CTP:{ 1, 90, 180, 245, 310, 375, 440, 500, 560, 620, 680, 740, 800, 875, 950, 1100} [hPa].

CTT:{ 200, 210, 220, 230, 235, 240, 245, 250, 255, 260, 265, 270, 280, 290, 300, 310, 350} [K]

5.2.4 Cloud Phase [CPH]

Similarly to CFC, the daily averages of CPH are calculated by temporal averaging of retrieval results on original pixel basis and subsequent remapping. CPH is expressed as fraction of

liquid water clouds by calculating the ratio of number of detected liquid clouds $N(i,j)_{Cloudy}$ with respect to the total number detected clouds $N(i,j)_{Cloudy}$:

Equation 5-4
$$CPH(i,j) = \frac{N(i,j)_{liquid}}{N(i,j)_{Cloudy}}$$

Cloud Phase is also provided as separate daytime and night-time averages.

The monthly mean CPH is calculated as mean over the daily means with each day being weighted equally.

The monthly CPH product also includes a one-dimensional monthly histogram. The CPH histogram includes temporally averaged number of occurrences of different cloud types. The bins in the CPH histogram correspond to the cloud types defined in Section 4.4:

CPH_bins: {0,1,2,3,4,5,6,7,8,9}.

Cloud types: {clear, not_used, not_used, water, supercooled, not_used, opaque_ice, cirrus, overlap, overshooting_convection}.

Possibly sunglint-affected pixels, for which microphysical cloud property retrievals may be impacted, are excluded from the CPH averaging. These pixels are defined by a scattering angle differing less than 27 degrees from the direct glint angle over water surfaces and a satellite viewing zenith angle larger than 30 degrees.

5.2.5 Liquid Water Path [LWP]

Daily mean LWP is calculated for each grid cell <LWP(i,j)> as given in Equation 5-2. Liquid clouds COT, CRE, CDNC and CGT are aggregated in the same way, and provided as additional data layers. Furthermore, for COT a logarithmic average is included, which is more consistent with the cloud radiative effect.

In addition to the in-cloud averages, all-sky LWP is calculated by a weighting of the LWP with the CFC including cloud-free and ice-cloud pixels as zeroes in the averaging.

The in-cloud and all-sky monthly mean LWP as well as the monthly mean of COT, CRE, CDNC and CGT of liquid clouds are calculated as mean over the daily means with each day being weighted equally.

One-dimensional histograms are generated for LWP and for COT, CRE, CDNC and CGT of liquid clouds on the same spatial resolution, but only on monthly basis. These histograms are described in a 4-dimensional field *LWP(i,j,bin,ph).* Indices *i* and *j* refer to location space, while *bin* is the index for specific bins of the range of occurring values, and *ph* denotes the cloud phase. Practically, these histograms are included in the liquid dimension of the CWP, COT, CRE, CDNC, CGT histograms with the following bin borders:

COT: {0.0, 0.3, 0.6, 1.3, 2.2, 3.6, 5.8, 9.4, 15.0, 23.0, 41.0, 60.0, 80.0, 149.99, inf}

CRE: {3, 6, 9, 12, 15, 20, 25, 30, 40, 60} [µm].

CDNC: {0, 2, 5, 10, 20, 50, 100, 150, 200, 300, 500, inf} [cm-3]

CGT: {0, 50, 100, 150, 250, 350, 500, 700, 1000, 1500, 2000, inf} [m].

CWP: {0, 5, 10, 20, 35, 50, 75, 100, 150, 200, 300, 500, 1000, 2000, inf} [g/m²]

Note that, as explained in Section 5.2.2, COT can in principle acquire arbitrarily large values and therefore the upper histogram bin was chosen to extend to infinity. The same is true for CWP, CDNC and CGT, since these are proportional to COT to some power.

Note: CDNC and CGT are retrieved for liquid clouds only but contain a phase dimension for consistency.

As satellite pixels with high surface albedo (e.g. by snow) are problematic for the retrieval of the properties mention in this section, the daily and monthly mean files contain an additional data layer providing the fractional occurrence of those pixels in a L3 grid cell. For LWP files these data represent liquid cloud cases only.

Possibly sunglint-affected pixels are excluded before LWP, COT, CRE, CDNC and CGT are aggregated to daily means, as described in Section 5.2.4. Additionally, CRE values are excluded from the averaging if the satellite-observed reflectances are located outside the look-up table (see Section 4.5).

5.2.6   Ice Water Path [IWP]

Daily mean IWP, as well as the ice cloud COT and CRE, are calculated in exactly the same way as LWP. This includes the computation of all-sky IWP and COT by including cloud-free and liquid-cloud pixels as zeroes in the averaging.

The in-cloud and all-sky monthly mean IWP as well as the monthly mean of COT and CRE of ice clouds are calculated as mean over the daily means with each day being weighted equally.

One-dimensional histograms are generated for IWP and for COT and CRE of ice clouds on the same spatial resolution, but only on monthly basis. Practically, these histograms are included in the ice dimension of the CWP, COT and CRE histograms with the following bin borders:

CWP: {0, 5, 10, 20, 35, 50, 75, 100, 150, 200, 300, 500, 1000, 2000, inf} [g/m²]

COT: {0.0, 0.3, 0.6, 1.3, 2.2, 3.6, 5.8, 9.4, 15.0, 23.0, 41.0, 60.0, 80.0, 149.99, inf}

REF: {3, 6, 9, 12, 15, 20, 25, 30, 40, 60} [µm].

As for LWP (see previous section) the fractional occurrence of ice cloud pixels with high surface albedo (e.g. by snow) are reported in each L3 grid cell in the IWP products. Also possibly sunglint-affected pixels and failed CRE retrievals are excluded before aggregation to daily means in the same way as for LWP.

5.3 Additional statistical parameters

In addition to the daily and monthly mean values, the standard deviations s over all valid and used values is calculated for CFC, CPH, CTO, LWP and IWP for each grid box with

Equation 5-5

$$\sigma_{std}^2 = \frac{1}{N} \sum_{i=1}^{N} (x_i - \langle x \rangle)^2$$

5.4 Uncertainty propagation

The propagation of CTP, CTH, CTP, COT, CRE, LWP and IWP uncertainties into level-3 products is implemented following Stengel et al. (2017). To recall, the reported pixel-based uncertainties σ_x for a given variable x represent the 68% confidence interval that the true value is within $x \pm \sigma_x$ This confidence interval can be propagated into daily mean level-3 products. For this, the standard deviation (Equation 5-5), the daily mean uncertainty (Equation 5-6) and the daily mean squared uncertainty (Equation 5-7) were calculated using the same pixels used for the calculation of the daily mean (Number: N, pixel index: i). Using Equation 5-8 the natural variability of a property can be determined, and Equation 5-9 reports how the uncertainty of the mean ($\sigma_{\langle x \rangle}$) can then be calculated. Note, that the uncertainty correlation c needs to specified. As this is usually not know, we used c=0.1 and c=1.0 to reflect two rather extreme scenarios. Thus, the uncertainties of the daily means are given for both uncertainty correlation estimates and again presents the confidence interval $\langle x \rangle \pm \sigma_{\langle x \rangle}$ in which the true mean lies with a confidence of 68% around the mean.

Equation 5-6

$$\langle \sigma_i \rangle = \frac{1}{N} \sum_{i=1}^{N} (\sigma_i)$$

Equation 5-7

$$\langle \sigma_i^2 \rangle = \frac{1}{N} \sum_{i=1}^{N} (\sigma_i^2)$$

Equation 5-8

$$\sigma_{natural}^2 = \sigma_{std}^2 - (1 - c)\langle \sigma_i^2 \rangle$$

Equation 5-9

$$\sigma_{\langle x \rangle}^2 = \frac{1}{N} \sigma_{natural}^2 + c\langle \sigma_i \rangle^2 + (1 - c)\frac{1}{N}\langle \sigma_i^2 \rangle$$

Based on the rationale above for daily mean products, the uncertainties for monthly mean products can be determined equivalently by replacing σ_i, which was the pixel-based (level-2) uncertainty, with $\sigma_{\langle x \rangle}$, which is the uncertainty of the daily mean, in Equation 5-5 to Equation 5-9 to express the uncertainty of the monthly mean ($\sigma_{\langle \langle x \rangle_j \rangle}^2$); see Equation 5-10, with M being the number of daily means available.

Equation 5-10
$$\sigma^2_{\langle\langle x\rangle_j\rangle} = \frac{1}{M}(\sigma_{\langle x\rangle})^2_{std} + c\langle(\sigma_{\langle x\rangle})_j\rangle^2 + (1-c)\frac{1}{M}\langle(\sigma_{\langle x\rangle})^2_j\rangle$$

An uncertainty correlation has to be specified for the uncertainties of the monthly means as well, and this done as for the daily means. Thus, two scenarios $c=0.1$ and $c=1.0$ were implemented with both using the daily mean uncertainty at $c=0.1$ as input.

5.5   Monthly mean diurnal cycles

To facilitate the assessment of monthly mean diurnal cycle for the user not only daily and monthly means are created but also monthly mean diurnal cycles from the quantities CFC, CTO, LWP, IWP and CPH. For a monthly mean diurnal cycle, all fields of a specific slot are considered and averaged hour wise, the result is a file with 24 fields. Each field contains the monthly average of all input fields of a specific hour (including 4 time slots per hours: '00, '15, '30, '45). Please note that the time axis refers to UTC; for a depiction in local time the pixel will have to be sorted with respect to the time zones.

6 References

Baum, B. A., P. Yang, A. J. Heymsfield, C. G. Schmitt, Y. Xie, A. Bansemer, Y.-X. Hu, and Z. Zhang, 2011: Improvements in shortwave bulk scattering and absorption models for the remote sensing of ice clouds, J. Appl. Meteorol. Clim., 50, 1037-1056, doi:10.1175/2010JAMC2608.1.

Bennartz, R. and J. Rausch, 2017: Global and regional estimates of warm cloud droplet number concentration based on 13 years of AQUA-MODIS observations, Atmos. Chem. Phys., 17, 9815-9836, doi:10.5194/acp-17-9815-2017.

De Haan, J. F., P. Bosma, and J. W. Hovenier, 1987: The adding method for multiple scattering calculations of polarized light, Astron. Astrophys., 183, 371-391.

Doelling, D. R., L. Nguyen, and P. Minnis, 2004: Calibration comparisons between SEVIRI, MODIS, and GOES data. In Proceedings of the 2004 EUMETSAT Meteorological Satellite Conference, Prague, Czech Republic. EUMETSAT.

EUMETSAT, 2017: MSG Level 1.5 Image Data Format Description, EUM/MSG/ICD/105 v8.

EUMETSAT, 2007: A Planned Change to the MSG Level 1.5 Image Product Radiance Definition, EUM/OPS-MSG/TEN/06/0519.

Ham, S.-H. and B. J. Sohn, 2010: Assessment of the calibration performance of satellite visible channels using cloud targets: application to Meteosat-8/9 and MTSAT-1R. Atmospheric Chemistry and Physics, 10(22), 11131–11149.

Håkansson, N. and Adok, C. and Thoss, A. and Scheirer, R. and Hörnquist, S. (2018) Neural network cloud top pressure and height for MODIS. Atmospheric Measurement Techniques. doi: 10.5194/amt-11-3177-2018

Karlsson, K.-G., E. Johansson and A. Devasthale, 2015: Advancing the uncertainty characterisation of cloud masking in passive satellite imagery: Probabilistic formulations for NOAA AVHRR data, Rem. Sens. Env., 158, 126-139; doi:10.1016/j.rse.2014.10.028.

Karlsson, K.-G., E. Johansson, N. Håkansson, J. Sedlar, S. Eliasson, 2020: Probabilistic Cloud Masking for the Generation of CM°SAF Cloud Climate Data Records from AVHRR and SEVIRI Sensors. Remote Sens.12, 713. https://doi.org/10.3390/rs12040713

Meirink, J.F., R.A. Roebeling and P. Stammes, 2013: Inter-calibration of polar imager solar channels using SEVIRI, Atm. Meas. Tech., 6, 2495-2508, doi:10.5194/amt-6-2495-2013.

Nakajima, T., and M. D. King, 1990: Determination of the Optical Thickness and Effective Particle Radius of Clouds from Reflected Solar Radiation Measurements. Part 1: Theory. J. Atmos. Sci ., 47, 1878-1893.

Pfreundschuh, S. and Eriksson, P. and Duncan, D. and Rydberg, B. and Håkansson, N. and Thoss, A. (2018) A neural network approach to estimating a posteriori distributions of Bayesian retrieval problems. Atmospheric Measurement Techniques. doi: 10.5194/amt-11-4627-2018. url: https://www.atmos-meas-tech.net/11/4627/2018/

Schmid, J., 2000: "The SEVIRI instrument." Proceedings of the 2000 EUMETSAT Meteorological Satellite Data User's Conference, Bologna, Italy, 29 May–2 June 2000.

Stengel, M., Stapelberg, S., Sus, O., Schlundt, C., Poulsen, C., Thomas, G., Christensen, M., Carbajal Henken, C., Preusker, R., Fischer, J., Devasthale, A., Willén, U., Karlsson, K.-G., McGarragh, G. R., Proud, S., Povey, A. C., Grainger, R. G., Meirink, J. F., Feofilov, A., Bennartz, R., Bojanowski, J. S., and Hollmann, R.: Cloud property datasets retrieved from AVHRR, MODIS, AATSR and MERIS in the framework of the Cloud_cci project, Earth Syst. Sci. Data, 9, 881-904, https://doi.org/10.5194/essd-9-881-2017, 2017.

Stephens, G. L., 1978: Radiation profiles in extended water clouds: II. Parameterization schemes. J. Atmos. Sci., 35, 2123-2132.

Yang, P., L. Bi, B. A. Baum, K.-N. Liou, G. W. Kattawar, M. I. Mishchenko, and B. Cole, 2013: Spectrally consistent scattering, absorption, and polarization properties of atmospheric ice crystals at wavelengths from 0.2 to 100 μm, J. Atmos. Sci., 70, 330-347, doi:10.1175/JAS-D-12-039.1.

7 Acronyms

ATBD	Algorithm Theoretical Baseline Document
AVHRR	Advanced Very High Resolution Radiometer
CALIOP	Cloud-Aerosol Lidar with Orthogonal Polarization
CDOP	Continuous Development and Operations Phase
CFC	Fractional Cloud Cover
CLAAS	CM SAF cLoud dAtAset using SEVIRI
CM SAF	Satellite Application Facility on Climate Monitoring
CDNC	Cloud Droplet Number Concentration
CGT	Cloud Geometrical Thickness
COT	Cloud Optical Thickness
CPP	Cloud Physical Properties
CRE	Cloud particle Effective Radius
CTH	Cloud Top Height
CTO	Cloud Top product
CTP	Cloud Top Pressure
CTT	Cloud Top Temperature
CTTH	Cloud Top Temperature and Height product (general PPS product name of these three kinds of cloud top descriptions)
CWP	Cloud Water Path (combining both LWP and IWP)
DWD	Deutscher Wetterdienst (German MetService)
ECMWF	European Centre for Medium Range Forecast
ECV	Essential Climate Variable
ERA5	ECMWF Re-Analysis 5
EUMETSAT	European Organisation for the Exploitation of Meteorological Satellites
FCDR	Fundamental Climate Data Record
GCOS	Global Climate Observing System
ISCCP	International Satellite Cloud Climatology Project

IWP   Ice Water Path

JCH   Joint Cloud properties Histogram

KNMI   Koninklijk Nederlands Meteorologisch Instituut

LUT   Look-Up Table

LWP   Liquid Water Path

MODIS   Moderate Resolution Imaging Spectroradiometer

MSG   Meteosat Second Generation

NOAA   National Oceanic & Atmospheric Administration

NWC SAF   SAF on Nowcasting and Very Short Range Forecasting

NWP   Numerical Weather Prediction

OSI SAF   SAF on Ocean and Sea Ice

PRD   Product Requirement Document

PPS   Polar Platform cloud processing sofware (from NWC SAF)

PUM   Product User Manual

RTTOV   Radiative Transfer for TOVS

SEVIRI   Spinning Enhanced Visible and InfraRed Imager

SAF   Satellite Application Facility

SMHI   Swedish Meteorological and Hydrological Institute

WCRP   World Climate Research Programme